



ACADEMIC  
PRESS

Available online at [www.sciencedirect.com](http://www.sciencedirect.com)

SCIENCE @ DIRECT®

Journal of Solid State Chemistry 173 (2003) 350–354

JOURNAL OF  
SOLID STATE  
CHEMISTRY

<http://elsevier.com/locate/jssc>

## LaSrMnCoO<sub>6</sub>: a new cubic double perovskite oxide

J. Androulakis,<sup>a,b</sup> N. Katsarakis,<sup>a</sup> J. Giapintzakis,<sup>a,c,\*</sup> N. Vouroutzis,<sup>d</sup> E. Pavlidou,<sup>d</sup>  
K. Chrissafis,<sup>d</sup> E.K. Polychroniadis,<sup>d</sup> and V. Perdikatsis<sup>e</sup>

<sup>a</sup> *Institute of Electronic Structure and Laser, Foundation for Research and Technology—Hellas, P.O. Box 1527,  
Vasilika Vouton, Heraklion, Crete 711 10, Greece*

<sup>b</sup> *Department of Chemistry, University of Crete, Leoforos Knossou, Heraklion, Crete 714 09, Greece*

<sup>c</sup> *Department of Materials Science and Technology, University of Crete, P.O. Box 2208, Heraklion, Crete 710 03, Greece*

<sup>d</sup> *Department of Physics, Aristotle University of Thessaloniki, Thessaloniki 54124, Greece*

<sup>e</sup> *Department of Mineral Resources Engineering, Technical University of Crete, University Campus, Chania 73100, Greece*

Received 12 August 2002; received in revised form 31 January 2003; accepted 13 February 2003

### Abstract

Single-phase polycrystalline powder samples of the double perovskite oxide LaSrMnCoO<sub>6</sub> were synthesized by the Pechini (citrate-gel) technique. The structural, magnetic and electrical properties of the obtained powders were investigated by X-ray diffraction, electron microscopy, dc magnetization, ac susceptibility and dc resistivity measurements. The crystal structure of the new compound was found to be cubic of space group  $Fm\bar{3}m$  at room temperature. Below 225 K, the samples exhibit ferrimagnetic behavior with a spin-glass-like character. Resistivity measurements indicate semiconducting behavior with two different conductivity mechanisms: thermally activated behavior below 190 K and variable range hopping above 190 K.

© 2003 Elsevier Science (USA). All rights reserved.

**Keywords:** Double perovskite; LaSrMnCoO<sub>6</sub>; Spin state transition; Spin glass; Co–Mn perovskite

### 1. Introduction

Double perovskites of the general formula  $A'A''B'B''X_6$ , where the ( $A'A''$ )-sites are occupied by rare or alkaline earth ions, ( $B'B''$ )-sites by transition metal ions and ( $X$ )-sites by oxygen or halide ions, have been known for several decades [1]. The study of these oxides was initiated in the 1950s and since then several hundred of these compounds have been produced and studied because they exhibit quite interesting structural, electronic as well as magnetic properties [2]. One can anticipate many more of this type of compounds to be realized given the diversity of the ions that can occupy both the  $A$  and  $B$ -sites. The last few years ordered double perovskite oxides ( $X=O$ ) have received an enormous amount of attention because certain members of this family of oxides exhibit spectacular physical

phenomena such as colossal magnetoresistance and half metallicity in the ferrimagnetic Sr<sub>2</sub>FeMoO<sub>6</sub> [3] and La<sub>2</sub>VRuO<sub>6</sub> [4] compounds.

The physical properties of double perovskites are generally determined by the cations occupying the  $B'$ ,  $B''$  sites. Thus, special attention has been given to the factors that impact the  $B$ -site arrangement [2], namely the charge, size and electronic configuration of  $B$  cations as well as the  $A/B$  size ratio. Anderson et al. [2] have concluded that an ordered structure is most likely to be formed if the charge difference between  $B'$  and  $B''$  is two or higher. An exception to this condition is the case of LaCaMnCoO<sub>6</sub> [5]; this compound is ordered even though the  $B'-B''$  charge difference is 1. It is noteworthy to mention that, according to the authors of Ref. [5], the doubling of the unit cell and the subsequent  $B$ -site ordering in LaCaMnCoO<sub>6</sub> could only be observed by electron diffraction and not by powder X-ray diffraction (XRD), which indicates that the ordering does not extend throughout the whole sample.

Here we report on the synthesis, and the structural, magnetic and electrical properties of a new ordered double perovskite LaSrMnCoO<sub>6</sub>. The compound is

\*Corresponding author. Institute of Electronic Structure and Laser, Foundation for Research and Technology—Hellas, P.O. Box 1527, Vasilika Vouton, Heraklion, Crete 711 10, Greece. Fax: +30-2810-391305.

E-mail address: [giapintz@iesl.forth.gr](mailto:giapintz@iesl.forth.gr) (J. Giapintzakis).

found to be semiconducting with a cubic double perovskite structure, and exhibits ferrimagnetic behavior with a spin-glass-like character. We briefly discuss the possible origin of this magnetic phase.

## 2. Experimental part

LaSrMnCoO<sub>6</sub> powder samples were prepared by the Pechini (citrate-gel) method, using very-high-purity (99.999%, Aldrich) metal nitrates [La(NO<sub>3</sub>)<sub>3</sub>·6H<sub>2</sub>O, Co(NO<sub>3</sub>)<sub>2</sub>·6H<sub>2</sub>O, Sr(NO<sub>3</sub>)<sub>2</sub>] and high-purity Mn<sub>2</sub>O<sub>3</sub> (99%, Aldrich) as starting materials. The materials were first dissolved in water and then an appropriate mixture of citric acid and ethylene glycol was added to the solution. The gel formation was catalyzed by the addition of HNO<sub>3</sub>. The resulted gel was decomposed at 350°C and the acquired precursor powders were heated in air at 550°C for 5 days and then at 1000°C for 12 h to improve crystallinity.

Powder XRD patterns were recorded using a Rigaku (RINT 2000) diffractometer with monochromated CuKα<sub>1</sub> radiation. The electron diffraction and microscopy were performed on a JEOL 100CX transmission electron microscope (TEM) operating at 100 kV. The energy dispersive X-ray (EDX) analysis was performed in a JSM-840A Scanning Electron Microscope equipped with an EDS Oxford ISIS 300 analytical system. Dc magnetization and ac susceptibility measurements were performed on powder samples with an Oxford Instruments MagLab EXA magnetometer in the temperature range 1.8 ≤ *T* ≤ 360 K. Resistivity as a function of temperature was measured on bar-shaped polycrystalline pellets in a home-made apparatus using a standard 4-probe setup arrangement.

## 3. Results and discussion

### 3.1. Structural properties

Fig. 1 shows the XRD pattern of LaSrMnCoO<sub>6</sub> measured at room temperature. The difference between the observed and the calculated patterns is plotted at the top of Fig. 1. The peaks of the pattern, which are marked by vertical bar signs, are indexed on a cubic *Fm* $\bar{3}$ *m* lattice of a double perovskite with ordered Mn and Co atoms. Thus, we conclude that the obtained polycrystalline powders are single phase and free of any impurity phases within the resolution of the instrument.

The diffraction spectrum was refined with the Rietveld analysis [6] employing the Pearson VII function [7] in order to describe the peak shape (Table 1). As it is readily seen from Fig. 1 the calculated pattern is in excellent agreement with the observed one ( $\chi^2 = 1.97$ ). The obtained unit-cell lattice parameter *a* = 7.6891 Å is

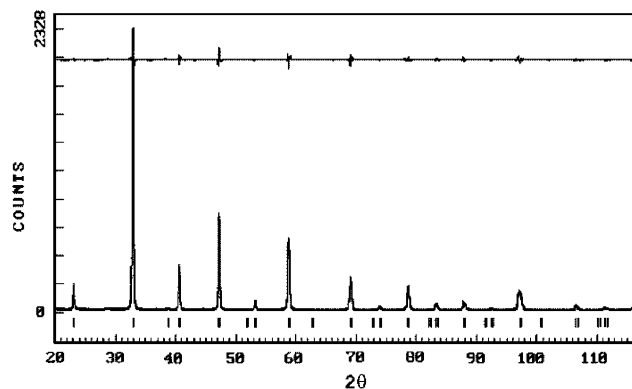


Fig. 1. X-ray powder diffraction pattern of LaSrMnCoO<sub>6</sub> measured at 297 K. The solid line at the top of the figure is the difference plot between the calculated and the measured profiles. The set of vertical bar marks at the bottom corresponds to the positions of the Bragg reflections.

Table 1  
Diffraction data collection conditions and refinement details for LaSrMnCoO<sub>6</sub> at 297 K

Space group	<i>Fm</i> $\bar{3}$ <i>m</i>
Refined lattice constant	7.6891(2) Å
Diffractometer	Rigaku (RINT 2000)
Geometry	Bragg–Brentano
Radiation	CuKα <sub>1</sub>
Counting Time	15 s/step
2θ range	15–120°
2θ step	0.02°
Profile function	Pearson VII
$R_{wp} = \left\{ \frac{\sum w_i (y_i(\text{obs}) - y_i(\text{calc}))^2}{\sum w_i y_i(\text{obs})^2} \right\}^{1/2}$	8.24%
$R_p = \frac{\sum  y_i(\text{obs}) - y_i(\text{calc}) }{\sum y_i(\text{obs})}$	8.60%
$R_F^a = \frac{\sum  (I_K(\text{obs})^{1/2} - I_K(\text{calc})^{1/2}) }{\sum (I_K(\text{obs}))^{1/2}}$	6.23%
$R_{Bragg}^a = \frac{\sum  I_K(\text{obs}) - I_K(\text{calc}) }{\sum I_K(\text{obs})}$	2.09%
$\chi^2$	1.97

<sup>a</sup>Note that *I<sub>K</sub>* is the intensity assigned to the *K*th Bragg reflection at the end of the refinement cycles.

slightly higher compared to the isostructural compound LaCaMnCoO<sub>6</sub> [5]. The atomic parameters, isotropic temperature factors and occupancies obtained from the refinement are listed in Table 2. The results of the Rietveld analysis, regarding the occupancies, were independently verified by EDX spectroscopy that showed the concentration ratio of [La<sup>3+</sup>]/[Sr<sup>2+</sup>] and [Mn]/[Co] cations to be 1 within the instrumental resolution ( $\pm 0.04$ ). It is noteworthy to point out the low value of the isotropic temperature factor for Co, (*B*<sub>ISO</sub> = 0.05), which implies scattering from Co-sites with different electronic density configuration and can be attributed either to different valence states or to different spin states of the Co cations occupying these sites. However, based on the EDX and magnetic

Table 2

Atomic parameters, isotropic temperature factors and occupancies of LaSrMnCoO<sub>6</sub> at 297 K. According to the occupancies the chemical formula is: La<sub>0.97</sub>Sr<sub>1.03</sub>MnCoO<sub>6</sub>

Atom	Wykoff site	x	y	z	<i>B</i> <sub>iso</sub>	Occupancy
La	8c	1/4	1/4	1/4	0.30	0.485
Sr	8c	1/4	1/4	1/4	0.28	0.514
Mn	4b	1/2	0	0	0.36	1
Co	4a	0	0	0	0.05	1
O	24e	0.2492(36)	0	0	1.48	1

Table 3

Bond lengths and angles calculated at 297 K

Bond	Bond length (Å)	Bond angle	Bond angle value (deg)
(La,Sr)–O	2.718	(La,Sr)–O–(La,Sr)	60.91 and 59.09
Mn–O	1.896	Mn–O–Mn	90
Co–O	1.949	Co–O–Co	90

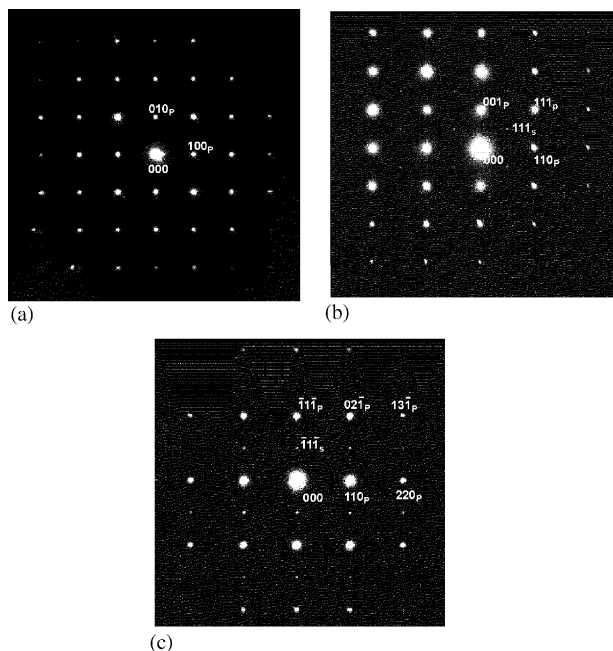


Fig. 2. Electron diffraction patterns of LaSrMnCoO<sub>6</sub> recorded with the beam parallel to: (a) [001], (b) [110], (c) [112] directions. In (b) and (c), superstructure reflections are observed due to doubling of the unit cell.

susceptibility (vide infra) results, we conclude that Co-sites are occupied by trivalent Co cations, which exhibit a random mix of spin states. Table 3 presents a summary of bond lengths and angles for all cations as extracted from the refinement procedure.

Fig. 2(a)–(c) shows three electron diffraction patterns taken along the [001], [110] and [112] zone axes, accessed by tilting experiments using a double-tilt specimen holder. In these patterns the main perovskite (*p*) spots are indicated, confirming a basic cubic structure. However, among these (*p*) indexed spots, some weak

intensity spots appear located in all the equivalent positions of half (111)<sub>p</sub> sites. The superstructure spots (*s*) provide clear evidence that the three sub-cell axes are doubled, in complete agreement with the results of the powder XRD studies. Although the observed area in TEM studies is always limited, repeated experiments carried out in different parts of the sample confirm the homogeneity of the powders.

### 3.2. Magnetic and electrical properties

The temperature dependence of the dc mass magnetization, measured in a field of 10 kOe, both under zero field cooled (ZFC) and field cooled (FC) conditions, is presented in Fig. 3. For temperatures below *T* ~ 225 K, we observe noticeable thermomagnetic irreversibility between the ZFC and FC curves, indicative of glassy behavior. The temperature dependence of the ZFC inverse molar susceptibility,  $\chi^{-1}(T)$ , is shown in Fig. 4. The shape of the  $\chi^{-1}(T)$  curve is characteristic of ferrimagnetic behavior. For *T* > 250 K the  $\chi^{-1}(T)$  data are fitted well to the Curie–Weiss law. The deduced value for the paramagnetic Curie temperature is  $\Theta = 61.39$  K and the effective number of Bohr magnetons is  $p_{\text{eff}} = 5.641 \mu_B$ .

The dc mass magnetization as a function of the applied magnetic field, *M*(*H*), at *T* = 1.8 K is depicted in Fig. 5. The hysteretic nature of the *M*(*H*) curve is consistent with the suggestion of ferrimagnetic behavior. The magnetization remains unsaturated even under the highest applied field (*H* = 60 kOe). Such behavior has been previously attributed to a high degree of spin disorder [8].

Ac susceptibility measurements,  $\chi_{\text{ac}}$ , were performed around the thermomagnetic irreversibility temperature with the driving ac field oscillating at three different frequencies, 669 Hz, 1 kHz and 1.631 kHz and with an amplitude of 1 Oe. Fig. 6 shows the temperature

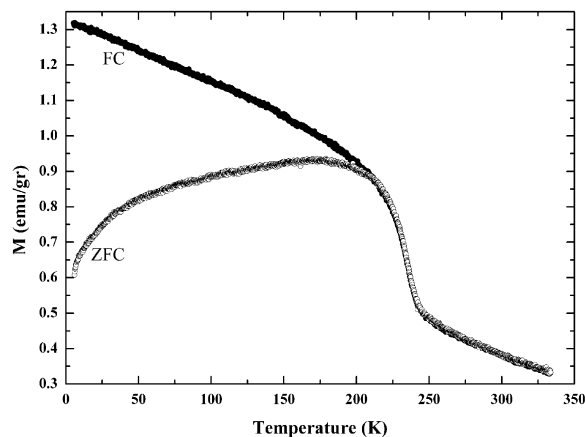


Fig. 3. Temperature dependence of mass magnetization of LaSrMnCoO<sub>6</sub> measured under a magnetic field of 10 kOe in ZFC and FC conditions.

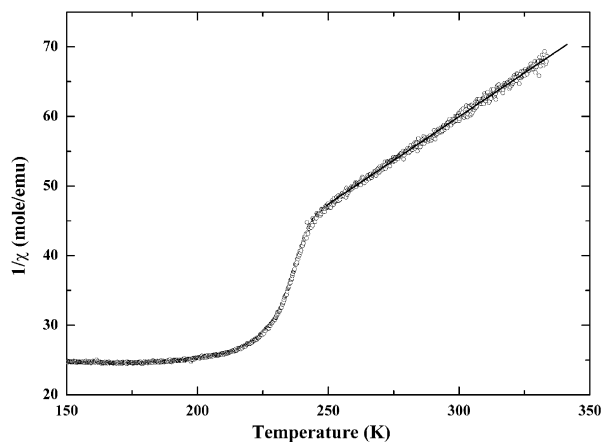


Fig. 4. Temperature dependence of inverse magnetic molar susceptibility of  $\text{LaSrMnCoO}_6$  measured under a magnetic field of 10 kOe. The line through the high temperature data points represents a fit to the Curie–Weiss law.

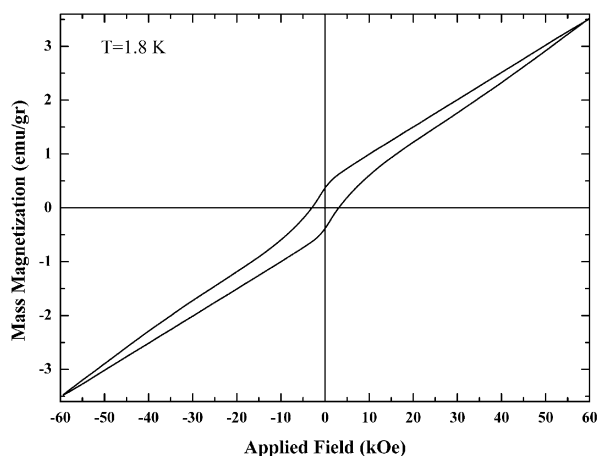


Fig. 5. Magnetic hysteresis loop of  $\text{LaSrMnCoO}_6$  measured at  $T = 1.8$  K.

dependence of the real part of the ac susceptibility in the temperature range  $210 < T < 250$  K. The amplitude of the peak appearing around 235 K is suppressed and its position is shifted towards higher temperatures with increasing frequency. Such behavior, in connection with the observed thermomagnetic irreversibility in dc magnetization mentioned previously, is consistent with the existence of spin-glass-like dynamics.

Given the fact that  $\text{LaSrMnCoO}_6$  is an ordered cubic perovskite, the origin of the spin-glass-like behavior can be traced to frustrated local magnetic interactions and in particular the existence of trivalent Co ions. Vallet-Regí et al., have reported that the oxidation states of the transition metals in  $\text{LaCaMnCoO}_6$  are  $4+$  and  $3+$  for Mn and Co, respectively [5]. In such a case second-order effects, such as temperature, may determine the spin state of octahedrally coordinated trivalent Co ions, since the intra-atomic exchange splitting and the crystal field splitting are approximately equal [9]. The majority of

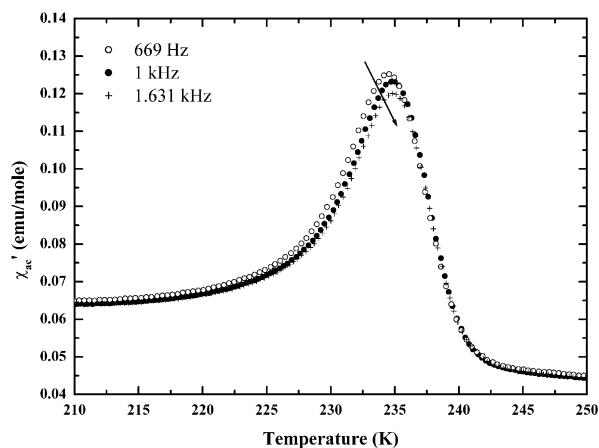


Fig. 6. Temperature dependence of the real part of the ac susceptibility,  $\chi'_{ac}(T)$ , of  $\text{LaSrMnCoO}_6$  for various frequencies of the ac driving field ( $h_{ac} = 1$  Oe) in zero bias dc field.

recent results on cobaltite perovskites points towards the following sequence of spin state transitions for the trivalent Co ions with increasing temperature: low (LS) to intermediate (IS) to high spin (HS) state [10]. Furthermore, there seem to be no data supporting a spin–orbit coupling in such perovskites, since crystal field effects are sufficient to relax the L–S coupling to a large extent. The aforementioned lead us to suggest that the experimentally determined  $p_{\text{eff}}$  is most likely the effect of the coexistence of two spin states of trivalent Co, namely IS and HS (see Table 4). Furthermore, since the thermally activated spin transition of trivalent Co ions is a statistical effect, it provides the basis for the development of random/frustrated  $\text{Mn}^{4+}$ – $\text{Co}^{3+}$  interactions.

Nevertheless, the sign of the aforementioned indirect exchange interactions is not trivial to predict. Qualitative superexchange rules, as suggested by Goodenough [11], address three types of cation–anion–cation interactions: (i) coupling between cations both with a half-filled  $e_g$  orbital leading to an antiferromagnetic spin arrangement (e.g.  $\text{LaFeO}_3$ ); (ii) coupling between a cation with a half-filled  $t_{2g}$  orbital and a cation with an empty  $e_g$  orbital, which is also antiferromagnetic (e.g.  $\text{LaCrO}_3$ ); and (iii) coupling between a cation with a half-filled  $e_g$  orbital and a cation with an empty  $e_g$  orbital, leading to parallel alignment of the cation spins and hence ferromagnetism (e.g.  $\text{La}_2\text{NiMnO}_6$ ). Case (iii) can account for a ferromagnetic  $\text{Co}^{3+}(\text{HS})$ – $\text{Mn}^{4+}$  interaction, which however, is not as clear as for example the  $\text{Ni}^{2+}$ – $\text{Mn}^{4+}$  case [12], where all the unpaired electrons lie on orthogonal orbitals (Ni  $e_g$  and Mn  $t_{2g}$ ). The orthogonality between the Ni  $e_g$  and Mn  $t_{2g}$  orbitals prohibits electronic transfer and as a consequence a ferromagnetic superexchange is stabilized. In addition, there are theoretical studies which indicate that superexchange interactions between cations with more than

Table 4

Calculated spin-only values for all  $\text{Co}^{3+}$  spin states. The experimentally determined value is  $5.641 \mu_B$

Oxidation states	Co spin configuration	Co total spin $S$	Spin only value $[\mu_{\text{Co}}^2 + \mu_{\text{Mn}}^2]^{1/2}$ , $\mu_i = [4S(S+1)]^{1/2}$
$\text{Mn}^{4+} (S = 3/2) \text{Co}^{3+}$	$t_{2g}^6 e_g^0$	0	3.873
	$t_{2g}^5 e_g^1$	1	4.796
	$t_{2g}^4 e_g^2$	2	6.245

five  $d$ -electrons should be antiferromagnetic [13] while interactions involving cations with less than five  $d$ -electrons (as in our case) could be either positive or negative depending on the specific  $A$  and  $B$  ions as well as the structure. The later case manifests most dramatically in  $\text{LaMnO}_3$ , where the  $a$ – $b$  plane interactions are ferromagnetic while alternating planes along the  $c$  direction are coupled antiferromagnetically giving rise to  $A$ -type antiferromagnetism. In view of the above, both  $(t_{2g}^4 e_g^2) - (t_{2g}^3 e_g^0)$  and  $(t_{2g}^5 e_g^1) - (t_{2g}^3 e_g^0)$  interactions (e.g., interactions between  $d^6$  and  $d^3$  cations) are quite unusual and, to the best of our knowledge, have never been reported before.

Given the fact that the investigated compound exhibits glassy ferrimagnetic behavior and is insulating (vide infra), i.e., no next nearest neighbor interactions could be mediated by itinerant carriers, the negative exchange coupling should be the result of an appreciable overlap of the orbitals of nearest neighbor cations ( $d^6$  and  $d^3$ ). Therefore it is clear, that the nature of interactions in  $\text{LaSrMnCoO}_6$  is quite complicated, revealing the necessity both for detailed electronic structure calculations as well as further experimental work to shed more light on the underlying physical mechanisms.

Fig. 7 presents the temperature dependence of the dc resistivity of  $\text{LaSrMnCoO}_6$ , which indicates that the synthesized compound is semiconducting. It is interesting to notice that the natural logarithm of the resistivity data above 190 K scales with  $T^{1/4}$  (see inset of Fig. 7), which is consistent with a variable range hopping (VRH) conductivity mechanism. On the other hand, at temperatures below 190 K, the resistivity curve suggests a thermally activated behavior of charge carriers (not shown here). Therefore, it is intriguing to suggest a possible connection between the randomly mixed IS-HS states of Co at  $B''$  and the observed VRH behavior of carriers close to the magnetic transition temperature.

In summary,  $\text{LaSrMnCoO}_6$ , a cubic ordered double perovskite oxide, has successfully been prepared and characterized. We have observed a magnetic transition around  $T_c \sim 225$  K, from a high temperature paramagnetic to a low temperature ferrimagnetic state. In addition, we have observed a spin-glass-like freezing of the moments below the ordering temperature and have attributed it to random interactions between  $\text{Mn}^{4+}$  and IS/HS octahedrally coordinated trivalent Co ions. Our

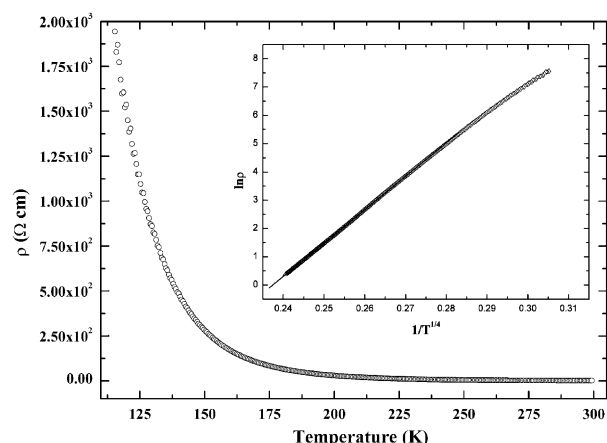


Fig. 7. Temperature dependence of the resistivity of  $\text{LaSrMnCoO}_6$ . Inset shows the  $\ln \rho$  vs.  $1/T^{1/4}$  plot for the same compound.

resistivity data show that the compound is semiconducting and exhibits VRH conductivity above  $\sim 190$  K and a thermally activated behavior of carriers at lower temperatures.

## References

- [1] I.N. Flerov, M.V. Gorev, K.S. Aleksandrov, A. Tressaud, J. Grannec, M. Couzi, Mater. Sci. Eng. 24 (1998) 81–151.
- [2] M.T. Anderson, K.B. Greenwood, G.A. Taylor, K.R. Poeppelmeier, Prog. Solid State Chem. 22 (1993) 197–233.
- [3] D.D. Sarma, Curr. Opin. Solid State Mater. Sci. 5 (2001) 261–268.
- [4] J.H. Park, S.K. Kwon, B.I. Min, Phys. Rev. B 65 (2002) 174401.
- [5] M. Vallet-Regi, E. García, J.M. Gonzalez-Calbet, J. Chem. Soc. Dalton Trans. 3 (1988) 775–779.
- [6] D.L. Bish, S.A. Howard, J. Appl. Cryst. 21 (1988) 86–91; S.A. Howard, RIQAS Rietveld Software, Department of Ceramic Engineering University of Missouri-Rolla, Rolla, MO.
- [7] R.A. Young, R.A. Young (Eds.), The Rietveld Method, Oxford University Press, Oxford, 1995, p. 9.
- [8] A. Chakravarti, R. Ranganathan, C. Bansal, Solid State Commun. 82 (1992) 591–595.
- [9] J.B. Goodenough, J. Phys. Chem. Solids 6 (1958) 287–297.
- [10] D. Louca, J.L. Sarrao, J.D. Thompson, H. Röder, G.H. Kwei, Phys. Rev. B 60 (1999) 10378–10382.
- [11] J.B. Goodenough, Magnetism and the Chemical Bond, Robert E. Krieger Publishing Company, New York, 1976, 170pp.
- [12] G. Blasse, J. Phys. Chem. Solids 26 (1965) 1969–1971.
- [13] P.W. Anderson, Phys. Rev. 79 (1950) 350–356; P.W. Anderson, Phys. Rev. 79 (1950) 705–710.